 Open access • Journal Article • DOI:10.1021/ACS.ENERGYFUELS.7B03242

Compositional characterization of pyrolysis fuel oil from Naphtha and vacuum gas oil

— [Source link](#) 

Nenad Ristic, Marko Djokic, Elisabeth Delbeke, Arturo González Quiroga ...+3 more authors





Institutions: Ghent University

Published on: 23 Jan 2018 - Energy & Fuels (American Chemical Society)

Topics: Fuel oil, Naphtha, Asphaltene, Gas chromatography and Flame ionization detector

Related papers:

- [Integrated hydrotreating and steam pyrolysis process for direct processing of a crude oil](#)
- [Integrated hydroprocessing and steam pyrolysis of crude oil to produce light olefins and coke](#)
- [Integrated hydrotreating and steam pyrolysis process including hydrogen redistribution for direct processing of a crude oil](#)
- [Integrated slurry hydroprocessing and steam pyrolysis of crude oil to produce petrochemicals](#)
- [Integrated hydroprocessing, steam pyrolysis and slurry hydroprocessing of crude oil to produce petrochemicals](#)

Share this paper:    

View more about this paper here: <https://typeset.io/papers/compositional-characterization-of-pyrolysis-fuel-oil-from-3qvr9vgscq>

1 Compositional Characterization of Pyrolysis Fuel 2 Oil from Naphtha and Vacuum Gas Oil

3 *AUTHORS' NAMES: Nenad D. Ristic¹, Marko R. Djokic¹, Elisabeth Delbeke^{1,2}, Arturo*
4 *Gonzalez-Quiroga¹, Christian V. Stevens², Kevin M. Van Geem¹, Guy B. Marin¹*

5 **AUTHORS' ADDRESS:**

6 1. Laboratory for Chemical Technology, Ghent University, Technologiepark 914, 9052 Ghent,
7 Belgium.

8 2. SynBioC, Department of Sustainable Organic Chemistry and Technology, Ghent University,
9 Coupure Links 653, 9000 Ghent, Belgium.

10 **KEYWORDS:** Steam Cracking, PAH, Aromatic hydrocarbons, NMR, GC × GC – FID/TOF-
11 MS.

12 **ABSTRACT**

13 Steam cracking of crude oil fractions gives rise to substantial amounts of a heavy liquid product
14 referred to as Pyrolysis Fuel Oil (PFO). To evaluate the potential use of PFO for production of
15 value-added chemicals a better understanding of the composition is needed. Therefore, two
16 PFO's derived from naphtha (N-PFO) and Vacuum Gas Oil (V-PFO) were characterized using
17 elemental analysis, SARA fractionation, nuclear magnetic resonance (NMR) spectroscopy and

1 comprehensive two-dimensional gas chromatography (GC × GC) coupled to a flame ionization
2 detector (FID) and time-of-flight mass spectrometer (TOF-MS). Both samples are highly
3 aromatic, with molar hydrogen-to-carbon (H/C) ratios lower than 1 and with significant content
4 of compounds with solubility characteristics typical for asphaltenes and coke, *i.e.* n-hexane
5 insolubles. The molar H/C ratio of V-PFO is lower than the one measured for N-PFO, as
6 expected from the lower molar H/C ratio of the VGO. On the other hand, the content of n-hexane
7 insolubles is lower in V-PFO compared to the one in N-PFO, *i.e.* 10.3 ± 0.2 wt.% and 19.5 ± 0.5
8 wt.%, respectively. This difference is attributed to the higher reaction temperature applied during
9 naphtha steam cracking, which promotes the formation of poly-aromatic cores and at the same
10 time scission of aliphatic chains. The higher concentrations of purely aromatic molecules present
11 in N-PFO is confirmed via NMR and GC × GC – FID/TOFMS. The dominant chemical family
12 in both samples are diaromatics, with a concentration of 28.6 ± 0.1 wt.% and 27.8 ± 0.1 wt.% for
13 N-PFO and V-PFO, respectively. Therefore, extraction of valuable chemical industry precursors
14 such as diaromatics and specifically naphthalene is considered as a potential valorization route.
15 On the other hand, hydro-conversion is required to improve the quality of the PFO's before
16 exploiting them as a commercial fuel.

17 **1. INTRODUCTION**

18 Steam cracking is considered as one of the most important petrochemical processes due to its
19 predominance for the production of light olefins such as ethylene and propylene¹. In the steam
20 cracking process saturated hydrocarbons are broken down into smaller, mainly unsaturated,
21 hydrocarbons in a coil constructed of high-temperature resistant alloys suspended in the radiant
22 reactor of a gas fired furnace. Subsequently, the product stream is cooled down in the transfer

1 line heat exchanger (TLE), to minimize unwanted reactions of valuable products such as
2 ethylene, propylene and butadiene. Ethane, liquefied petroleum gas and naphtha are typically
3 used as feedstocks for steam cracking. Nevertheless, heavier feedstocks such as atmospheric and
4 vacuum gas oils (VGO) are possible alternatives. Compared to lighter feedstocks, steam cracking
5 of high-boiling point mixtures results in lower yields of light olefins, higher yields of steam
6 cracking by-products and higher fouling rates in the reactor and the TLE²⁻⁴. While pyrolysis
7 gasoline, containing primarily benzene, toluene and xylene, is straightforward to valorize, the
8 heavier by-products called steam cracking residue or pyrolysis fuel oil (PFO) are more difficult
9 to exploit. PFO, separated from valuable products via primary fractionation, is rich in poly-
10 aromatic molecules^{5, 6} which makes it attractive for the production of carbon black⁷ and for
11 naphthalene extraction⁸. More often, heavy PFO is used for blending and subsequently as an
12 industrial fuel, flux oil or bunker fuel. Depending on the feedstock and steam cracking severity,
13 the impact of PFO on the overall ethylene plant economy can be significantly different. The
14 amount produced varies considerably, *e.g.* 3.0-6.0 wt.% and 21.0-25.0 wt.% for naphtha and
15 VGO, respectively⁹. Knowledge of the precise chemical composition is fundamental for
16 assessing the valorization, integration possibilities, and the required downstream processing
17 steps. Most importantly an improvement of the molecular characterization of heavy reaction
18 products is a necessary step for optimization of the steam cracking process when heavy liquids
19 are used. In other words, it is a pre-requirement before one could even attempt modelling of
20 heavy hydrocarbon mixture pyrolysis¹⁰. Additionally, identification and quantification of heavy
21 poly-aromatics is in particularly important for improving the understanding of coke formation
22 during steam cracking of hydrocarbons. Heavy poly-aromatics are considered as some of the
23 main coke precursors in both the reactor and the TLE of a steam cracker¹¹. Moreover,

1 compositional characterization of the stream is a requirement for optimizing downstream
2 processes. A recurrent problem is the gum formation via polymerization, which causes
3 incomplete combustion when the stream is utilized as a fuel. Finally, environmental concerns
4 drive the industry towards molecular characterization, since several compounds are highly
5 carcinogenic¹².

6 Despite the increasing importance of compositional characterization promoted by so-called
7 molecular based management^{13, 14}, methodologies employed by the mayor oil and petrochemical
8 companies, detailed results for PFO are scarce or unavailable in open literature due to difficulties
9 in performing experiments on relevant steam cracking conditions, producing sufficient sample
10 quantities and challenging sample preparation procedures. Moreover, the poly-aromatic nature of
11 the mixture requires the development of methods able to resolve the complicated PFO matrix.

12 Fast scanning of heavy hydrocarbon mixtures, *i.e.* heavy crude oil, bitumen¹⁵, sand oil¹⁶ and even
13 asphaltenes¹⁷, can be achieved via Direct Insertion Probe-Mass Spectrometry (DIP-MS).

14 Discrimination of heavy molecules is avoided by a program evaporation under vacuum
15 conditions and direct transfer towards the MS. Therefore, the DIP-MS method enables finger-
16 printing of samples and a rough separation based on volatility. Nevertheless, the separation
17 resolution is limited and the quantification via MS is challenging due to an enormous calibration
18 effort¹⁸. On the other hand, gas chromatography provides higher resolution for the
19 characterization of poly-aromatic hydrocarbons^{12, 19}. In particular comprehensive two-
20 dimensional gas chromatography (GC × GC) is a superior characterization technique for
21 characterization of petroleum-derived samples compared to one dimensional GC²⁰⁻²³. Dutriez et
22 al.^{24, 25} developed a GC × GC method for quantitative analysis of heavy hydrocarbons with
23 carbon numbers up to C₆₀, and subsequently optimized the method to characterize vacuum resin

1 fractions without discrimination in the injector²⁶. However, the detailed composition could not be
2 obtained due to substantial co-elution of different compounds. On the other hand, Fourier
3 Transform Ion Cyclotron Resonance Mass Spectrometry (FT-ICR-MS) showed that GC methods
4 do not characterize all the heavy poly-aromatic compounds in coal tar²⁷. Even though high
5 resolution FT-ICR-MS enables accurate determination of the molecular mass and chemical
6 nature of heavy compounds²⁸⁻³⁰, accurate quantification remains a challenge^{31, 32}. Complicated
7 sample matrices can alternatively be analyzed via Nuclear Magnetic Resonance (NMR)
8 spectroscopy, which provides information on the relative abundance of chemical families^{33, 34}.
9 Similarly, poly-aromatic compounds can be separated using liquid chromatography³⁵⁻³⁸;
10 nevertheless, the developed methods are time consuming and still primarily qualitative. Due to
11 the inherent limitations of each discussed analytical method only a combination of different
12 analytical techniques can result in quantitative characterization of fractions such as PFO.

13 In this work we have for the first time characterized PFO samples produced during steam
14 cracking of naphtha and VGO. Elemental analysis, SARA (saturates, aromatics, resins and
15 asphaltenes) fractionation, NMR and GC × GC coupled with Time of Flight Mass Spectroscopy
16 (TOF-MS) and Flame Ionization Detector (FID) allowed characterization and comparison
17 between two potentially very different PFO samples. Finally, guidelines for further processing of
18 heavy steam cracking products are given based on the performed detailed characterization.

19 **2. EXPERIMENTAL SECTION**

20 **2.1. Chemicals**

21 Analytical gases (helium, oxygen, nitrogen, hydrogen and air) used for elemental analysis and GC
22 × GC have a minimal purity of 99.99% (Air Liquide, Belgium). 3-chlorothiophene, used as internal

1 standard in GC × GC analyses, has a purity of 98% (Sigma-Aldrich, Belgium). 2-chloropyridine,
2 used as a secondary internal standard in GC × GC analyses has a purity of 99% (Sigma-Aldrich,
3 Belgium). Carbon disulfide used as a solvent for GC × GC analyses was supplied with a 99.9%
4 purity (Sigma-Aldrich, Belgium). The purity of deuterated chloroform, the solvent used for NMR
5 analysis, is 99.8 % (Sigma-Aldrich, Belgium). A standard Poly-nuclear Aromatic Hydrocarbons
6 (PAH) mixture supplied by Sigma-Aldrich (Belgium, CRM47543) was used for GC × GC method
7 development. Dichloromethane (DCM) used for extraction of heavy organic reaction by-products
8 was supplied with a 98% purity (Chem-Lab, Belgium). DCM and n-hexane used for SARA
9 fractionation (Sigma-Aldrich, Belgium) are HPLC grade. Steam used as a diluent in cracking
10 experiments was produced by superheating of water demineralized over an ion exchange column.

11 **2.2. Steam cracking feedstocks**

12 Two different crude oil fractions, naphtha and vacuum gas oil (VGO), were tested as steam
13 cracking feedstocks. These feedstocks were provided by Total (Antwerp, Belgium) and some of
14 their global characteristics are given in Table 1. The boiling point curve was determined using an
15 ASTM D1160 distillation unit (B/R instruments, USA) at atmospheric pressure for naphtha and
16 at a reduced pressure of 0.13 kPa for VGO. Elemental (CHNS & O) and PINA (paraffins,
17 isoparaffins, naphthenes, aromatics) compositions were obtained using the method developed by
18 Dijkmans et al.³⁹.

19 **Table 1.** Elemental composition, molecular family mass percentage and boiling point curve of
20 naphtha and VGO.

21

1 2.3. Pilot plant steam cracking experiments

2 Steam cracking experiments were performed in the pilot plant steam cracker (Laboratory for
3 Chemical Technology, Ghent University, Ghent, Belgium) which is described in detail
4 elsewhere^{40, 41}. An Incoloy 800HT reactor (12.8 m, 9 mm I.D.) is suspended in the gas-fired
5 furnace divided into five separate cells, in which the temperature is independently controlled by
6 regulating the fuel supply. Twenty thermocouples and five manometers are located along the
7 reactor coil. The pilot plant effluent is sampled on-line at high temperature (673 K - 773 K) using
8 a valve-based sampling system and an uniformly heated transfer line^{40, 42}. Downstream, the
9 steam cracking effluent enters the TLE from the top side and is cooled at controlled temperature.
10 Namely, TLE temperature profile is controlled by regulating the flowrate of the co-currently fed
11 cooling air and by setting the temperature in three independent heating zones.

12 Downstream of the TLE, the effluent stream is cooled to 353 K using an oil cooler heat
13 exchanger. The gas stream containing the main reaction products, *i.e.* ethylene, propylene and
14 butadiene, is sent to the flare connected to the vent line. On the other hand, water and cracking
15 by-products, PFO and a fraction of pyrolysis gasoline, are condensed and collected in a knock-
16 out drum. Subsequently, the mixture is transferred into a sampling vessel via transfer line kept at
17 373 K in order to prevent solidification of heavy reaction products. The interested reader is
18 referred to the Supplementary Information for a schematic description of the steam cracking pilot
19 plant.

20 Naphtha was cracked at a coil outlet temperature of 1123 K, coil outlet pressure of 170 kPa,
21 steam dilution ratio of 0.5 kg/kg. Conversely, VGO was cracked at a coil outlet temperature of
22 1073 K, coil outlet pressure of 170 kPa and steam dilution ratio of 1.0 kg/kg. For both cases the

1 TLE outlet temperature was kept at 673 K. These operating conditions are generally applied for
2 cracking of similar feedstocks^{2, 9, 10, 43}.

3 **2.4. Sample preparation procedure**

4 Heavy reaction products, *i.e.* a collected mixture of pyrolysis gasoline, PFO and water (see
5 section 2.3.), were mixed and transferred to three identical vessels with a volume of 1 L. In the
6 following step, 200 mL of the mixture was mixed with 100 mL of DCM and kept for two hours
7 in a 500 mL borosilicate glass separation funnel. After complete separation of the phases, the
8 DCM extract was transferred to a 2 L collecting vessel. Subsequently, approximately 500 mL of
9 the extract was transferred to a 1 L vessel connected to a rotary evaporator. The water residue,
10 compounds with lower boiling point considered as pyrolysis gasoline and the solvent, *i.e.* DCM
11 were evaporated at 353 K and 5 kPa. The obtained hydrocarbon residue is considered as the PFO
12 sample.

13 **2.5. Analytical Methods**

14 **2.5.1. Elemental analysis**

15 Thermo Scientific™ FLASH 2000 Series Elemental Analyzer (EA) (Interscience, Belgium)
16 equipped with a Thermal Conductivity Detector is used for determination of the elemental
17 composition. The solid cup injection technique is chosen to avoid injection discrimination of
18 PFO samples (see section 2.4.). The uncertainties on the detected amounts of carbon, hydrogen
19 and oxygen were within vendor specifications. The elemental composition is based on three
20 repeated analyses. The summations of CHNSO mass percentages were always within 97 and
21 103%.

1 2.5.2. SARA fractionation

2 Fractionation was initiated by keeping the PFO samples (see section 2.4.) under an 1 L min⁻¹
3 nitrogen flow, temperature of 333 K and pressure of 5 kPa for 72 hours. The mass evaporated
4 during that period was considered as a topping loss. After evaporation of all light compounds, n-
5 hexane insolubles, further considered as asphaltenes and coke, precipitated from the rest of the
6 hydrocarbon matrix. 210-250 mg of the sample was filtered after dissolving in 1 mL of n-hexane.
7 Asphaltenes and coke were later removed from the filter by dissolving them in DCM.
8 Subsequent separation of fractions referred to as saturates, aromatics and resins was performed
9 on a mid-pressure liquid chromatography (MPLC) system (Köhnen-Willsch, Jülich, Germany).
10 The dissolved fraction was injected into a pre-column filled with deactivated fine silica (63-200
11 µm) and deactivated coarse silica (200-500 µm). A flow of 2.4 mL min⁻¹ of n-hexane was
12 constantly fed to the pre-column for 450 s flushing the saturate and aromatic fractions into the
13 main column. On the other hand, the resin fraction remained on the pre-column. Subsequently,
14 saturate and aromatic fractions were separated in the main column filled with fine deactivated
15 silica (40-63 µm) and the saturate fraction was collected after 180 s. Next, the pre-column was
16 removed and the main column back-flushed for 450 s with an increased n-hexane flow of 3.0 ml
17 min⁻¹, thus enabling the elution of the aromatic fraction. A Refractive Index Detector and
18 Ultraviolet Detector were used to monitor the elution of the above-mentioned fractions. The resin
19 fraction trapped on the silica packing of the pre-column was separated by dissolving it in DCM
20 and filtering of the silica. Finally, saturate and aromatic fractions were placed in a vaporizer
21 where at 303 K and air flow of 70 ml min⁻¹ the majority of the n-hexane was removed. The
22 residue was washed with DCM and transferred to a weighted vial. Each fraction was placed in

1 the fume hood over night to evaporate DCM. In the last step, the vials were weighted and the
2 masses of each separated fraction determined.

3 **2.5.3. NMR**

4 100 mg of each PFO sample (see section 2.4.) was dissolved in 1 mL of CDCl₃ (deuterated
5 chloroform) and filtered over cotton wool in a Pasteur pipette to remove all insoluble particles.
6 The cotton wool was rinsed until becoming colorless with an additional 0.2 mL of CDCl₃, and
7 the combined solvent fractions were dried under reduced pressure. The ¹³C-NMR spectra are
8 recorded on a 400 MHz NMR spectrometer (Bruker Avance III Nanobay) at a resonance
9 frequency of 100 MHz using a 5 mm broadband probe. The solvent signal of 77.16 ppm is used
10 as the internal reference. Using CDCl₃ as a solvent enables analyzing of the same sample via
11 proton NMR if necessary and furthermore secures accurate chemical shift locking. The ¹³C-
12 NMR spectra is acquired with 30° pulse angle, proton decoupling, sweep width of 24038.461
13 Hz, and corresponding acquisition time of 1.36 s. Acquisition of 2048 scans using a 8 s pulse
14 delay resulted in a good signal-to-noise ratio after 5.40 h of total time of measurement per
15 sample. All experiments were performed at 298 K. The spectra were processed using TopSpin
16 3.2 to perform baseline corrections and integrations.

17 The NMR spectra are interpreted according to the methodology initially developed by Solum et
18 al.⁴⁴ and later applied for kerogen characterization by Kelemen et al.³⁴. However, the dipolar
19 dephasing, which allows the separation of protonated and non-protonated aromatic carbons³⁴,
20 was not possible and thus the fraction of bridgehead non-protonated aromatic carbon and average
21 carbon number per aromatic were not calculated.

22 **2.5.4. GC × GC**

1 **2.5.4.1. Sample preparation**

2 Two samples of each PFO (see section 2.4) were prepared for analyses using GC × GC – FID,
3 and GC × GC – TOF-MS. 3-chlorothiophene and 2-chloropyridine were chosen as internal
4 standards for FID analysis. These internal standards were added to the PFO samples according to
5 the procedure described by Dijkmans et al.^{39, 45}. Finally, samples were diluted using carbon
6 disulfide in a 1:1 volumetric ratio to decrease the viscosity and inhomogeneity of the mixture.

7 **2.5.4.2. GC × GC set-ups**

8 All samples were analyzed on a Thermo Scientific TRACE GC × GC set-up (Interscience,
9 Belgium) equipped with a FID detector, a TOF-MS detector (Interscience, Belgium), a dual-
10 stage cryogenic (liquid CO₂) modulator and a Programmable Temperature Vaporization (PTV)
11 injector (Interscience, Belgium). An MXT-1 (Restek, 60 m, 0.25 mm, 0.25 μm) was used as the
12 first dimension column, while a BPX50 (SGE Analytical Science, 2 m, 0.15 mm, 0.15 μm) was
13 used as the second dimension column. The modulator and both columns were positioned together
14 in a single oven. The PTV temperature was increased from 313 K up to the maximum
15 temperature of 673 K with a rate of 10 K min⁻¹. The initial column temperature was 313 K and
16 was increased up to 643 K at a rate of 2 K min⁻¹ where the column was kept isothermally for 600
17 s. Modulation was carried out on a piece of deactivated column with a set modulation time of 15
18 s. The scan frequency of the FID was 100 Hz, while the acquisition frequency of the TOF-MS
19 was 30 Hz in a mass range of 15–400 amu. TOF-MS electron impact ionization was 70 eV and
20 the detector voltage was 1700 V. The interface between the GC × GC and the TOF-MS was set
21 at 553 K and the TOF-MS source temperature at 473 K. Optimal helium carrier gas flow of 2.1

1 ml min⁻¹ for FID and 2.6 ml min⁻¹ for TOF-MS is calculated according to the method of Beens et al.^{40, 46}.

3 2.5.4.3. Data acquisition and quantification

4 Thermo Scientific's Xcalibur software enabled acquisition and processing of GC × GC-TOF-MS
5 data. For the GC × GC-FID data Thermo Scientific's Chrom-Card data system was used. The
6 raw GC × GC-FID data was exported to a NetCDF file and subsequently processed by GC Image
7 (Zoex Corporation, USA). The obtained peaks were tentatively identified using two independent
8 parameters, *i.e.* cross referencing the measured TOF-MS spectra to the spectra available in the
9 MS libraries⁴⁷ and using Kovats retention indices. The blob names and peak volumes were
10 exported as a .csv file which was subsequently processed using an in-house macro file. The
11 quantification procedure described in Supplementary Information was based on the internal
12 standard method developed by Dijkmans et al.^{39, 48}.

13 3. RESULTS AND DISCUSSION

14 3.1. Elemental composition

15 Elemental compositions of both samples, PFO's obtained from naphtha (hereinafter referred to
16 as N-PFO) and vacuum gas oil steam cracking (hereinafter referred to as V-PFO) are shown in
17 Table 2. Molar hydrogen-to-carbon (H/C) ratios are lower than those reported for asphaltenes
18 from Arabian crude oils⁴⁹, however higher compared to those reported for coal tar⁵⁰. This is a
19 first indication of the pronounced aromatic nature of the samples.

20 **Table 2.** Comparison of the elemental composition of N-PFO and V-PFO.

1 Even though naphtha and VGO have significantly different carbon number distribution and
2 chemical composition (see Table 1), their respective PFO's do not differ considerably in H/C
3 ratio. However, a slightly lower value is determined for V-PFO, *i.e.* 0.93, compared to that for
4 N-PFO, *i.e.* 0.95. Due to the low nitrogen and sulfur content in the feedstocks, these elements
5 were on and under the method's detection limit, respectively. On the other hand, oxygen is
6 present in higher amounts, accounting for 1.8 wt.% of the N-PFO and 1.0 wt.% of the V-PFO,
7 respectively. These oxygen amounts suggest the presence of entrained water which was not
8 completely evaporated during the sample preparation step (see section 2.4).

9 High carbon content and low nitrogen and sulfur content make N-PFO and V-PFO a cheap raw
10 material for production of carbon black⁵¹. Moreover, a relatively low content of oxygen implies
11 that these fractions are favorable feedstocks for direct liquefaction⁵². Namely, the molar H/C
12 ratio is relatively high and would lead to high quality of products. Similarly, due to the beneficial
13 elemental composition, processes such as Fischer–Tropsch, in which PFO would be steam
14 reformed to synthesis gas and subsequently converted to liquid fuels could be considered.

15 **3.2. SARA fractionation**

16 Fractionation procedure exploiting the difference in solubility of large highly aromatic
17 compounds was used to measure the amount of non-volatile compounds in PFO samples.
18 Fractionation results are dependent on the applied procedure⁵³ and the nature of the sample.
19 However, results obtained under the same conditions for the samples of similar chemical
20 composition can be compared, and the amount of heavy PAH estimated. Table 3 shows the
21 marked poly-aromatic nature of both samples, *i.e.* the measured amounts of resins, asphaltenes
22 and coke are significant.

1 **Table 3.** SARA fractionation results for N-PFO and V-PFO.

2 The fraction of light compounds evaporated, *i.e.* topping losses, is higher for the N-PFO sample.
3 SARA fractionation analysis indicates that the content of aromatics is higher in the V-PFO. The
4 difference measured according to SARA fractionation is larger due to the higher concentration of
5 heavier poly-aromatics in V-PFO that do not evaporate under reduced pressure during sample
6 topping (see section 2.5.2). Furthermore, the amount of resins is also higher in the V-PFO
7 sample. On the other hand, the content of n-hexane insoluble fraction, defined as asphaltenes and
8 coke (potentially spalled off from the reactor and the TLE) is almost twice higher in N-PFO.
9 Intensified formation of asphaltenes and coke during naphtha cracking can be assigned to the
10 lower dilution and higher cracking temperature^{54, 55}.

11 The high concentration of asphaltenes might be the principle disincentive for downstream
12 processing due to potential equipment fouling. However, the content of resins, that serve as a
13 peptizing agents⁵⁶, and aromatics is high, making asphaltenes soluble^{57, 58}. As V-PFO has a
14 lower asphaltene content and higher amount of aromatics and resins compared to N-PFO, it is a
15 better candidate for further processing. Nevertheless, due to relatively high boiling point of
16 aromatic molecules and resins, the mixture will tend to solidify, thus steam heated lines need to
17 be used for material transfer after the primary fractionation unit.

18 **3.3. Chemical structure**

19 The chemical structure of the hydrocarbon compounds present in PFO is studied in detail using
20 ¹³C NMR. The spectra obtained for N-PFO and V-PFO are shown in figures, respectively.

21 **Figure 1.** ¹³C NMR spectrum of N-PFO.

1 **Figure 2.** ^{13}C NMR spectrum of V-PFO.

2 The relative quantities of the identified carbon atom types and the lattice parameters used for
3 characterization are shown in Table 4.

4 **Table 4.** ^{13}C NMR determined structural and lattice parameters of N-PFO and V-PFO.

5 Chemical shifts corresponding to phenoxy/phenolic (150-165 ppm), alcohol/ether (50-90 ppm)
6 and methoxy (50-60 ppm) structures are not detected. Similarly, chemical shifts in the range
7 from 165 to 240 ppm are not identified. This confirms the limited content of carboxyl, carbonyl
8 and amide groups. These results indicate that compounds containing carbon/oxygen bonds if
9 present, have a very low concentrations in the studied PFO samples below the method detection
10 limit, *i.e.* 0.3 wt.% of carbon. A more plausible explanation for the oxygen detected using
11 elemental analysis is presence of entrained water. The nature of the feedstock is the dominant
12 factor influencing the high aromatic to aliphatic carbon ratio of the N-PFO. However, the effect
13 is emphasized with lower dilution and higher cracking temperature that further promotes the
14 formation of aromatic cores⁴⁰. Similarly, higher cracking temperatures increase the formation of
15 methylene/methine (22-90 ppm - (50-60) ppm) as opposed to methyl groups (0-22 ppm), which
16 explains the marked difference in abundance between these chemical families for N-PFO. A high
17 aromatic content is confirmed for both samples, accounting for 92.1 wt.% and 89.0 wt.% of N-
18 PFO and V-PFO, respectively. Even though the aliphatic content in V-PFO is higher, the amount
19 of alkyl-substituted aromatic carbon (135-150 ppm) is lower compared to the one of N-PFO. The
20 latter seems unexpected as the presence of non-aromatic carbon is limited, however these two
21 observations indicate that scission of aliphatic side chain bonds is more pronounced during
22 naphtha cracking, as a consequence of higher cracking temperature. Furthermore, by evaluating

1 the ratio of the aliphatic content and the alkyl-substituted aromatic carbon content, it is possible
2 to estimate the average carbon chain length bonded to the aromatic core. The calculated values of
3 1.1 for N-PFO and 1.8 for V-PFO are thus in line with the higher cracking severity. Similarly, it
4 is possible to estimate the degree of branching, more specifically aromatic carbon with the alkyl
5 side chain, by dividing the measured amount of alkyl-substituted aromatic carbon with the total
6 aromatic content. This ratio shows that 8 wt.% of N-PFO aromatic carbon and 7 wt.% of V-PFO
7 aromatic carbon have side chain bonds.

8 **3.4. Detailed Chemical Composition by GC × GC**

9 The high boiling point of poly-aromatic compounds implies that not all the compounds present in
10 the PFO mixture will be detectable with gas chromatography. Therefore, the applied GC × GC
11 method is initially evaluated using a standard poly-aromatic hydrocarbon (PAH) mixture
12 (composition given in Table 5).

13 **Table 5.** Composition of the standard test mixture.

14 The standard mixture is analyzed at the conditions subsequently applied for characterization of
15 PFO samples as described in section 2.5.4.2. From the chromatogram shown in Figure 3, it can
16 be concluded that even poly-aromatic molecules with the highest boiling point in the standard
17 mixture, *i.e.* dibenz[a,h]anthracene (797 K) and Indeno[1,2,3-cd]pyrene (809 K), can be detected
18 and quantified. The complete separation of each compound is not achieved. Molecules with the
19 same carbon number, such as benzo[k]fluoranthene and benzo[b]fluoranthene are not separated
20 and the same holds for benzo[ghi]perylene and dibenz[a,h]anthracene. Consequently, such heavy
21 poly-aromatics (five fused aromatic rings) are quantified as a lump of molecules with the same
22 carbon number belonging to the same chemical family.

1 **Figure 3.** GC × GC-FID chromatogram of the PAH standard. Numbers correspond to the
2 compounds list in Table 5.

3 Therefore, the described methodology using GC × GC - TOF-MS and GC × GC - FID enables
4 qualitative and quantitative analysis of part of the PFO samples chemical nature. However, it
5 should be stressed that complete characterization of the samples was not possible. Indeed, the
6 internal standard method shows that 83.7 wt.% of the N-PFO and 92.1 wt.% of the V-PFO are
7 quantified. The higher content of the highly aromatic non-volatile molecules in N-PFO is in
8 agreement with SARA fractionation results which showed 19.5 wt.% and 10.5 wt.% of n-hexane
9 insoluble material for N-PFO and V-PFO, respectively. As shown in the chromatogram for N-
10 PFO in Figures 4 and that for V-PFO in Figure 5, the added internal standard compounds were
11 adequately separated from the other compounds in the resulting chromatograms. This was
12 verified by calculating the bi-dimensional resolution, which should be higher than unity⁵⁹ for an
13 adequate separation. In this case the bi-dimensional resolutions were 8.7 for 3-chlorothiophene
14 and 5.0 for 2-chloropyridine. The purpose of adding an internal standard was twofold, on the one
15 hand to determine the quantity of compounds present in the sample and on the other hand to
16 confirm that the homogeneity of the sample is adequate. Known quantities of both standards
17 were used for quantitative analysis and the same results were obtained within experimental
18 precision, which confirms that there was no phase separation within the prepared samples.

19 **Figure 4.** GC × GC-FID chromatogram of the N-PFO with separation of molecular families.

20 Numbers correspond to the compounds list in Table 4.

21 **Figure 5.** GC × GC-FID chromatogram of the V-PFO with separation of molecular families.

22 Numbers correspond to the compounds list in Table 4.

1 The nature of compounds in both samples is aromatic, however the carbon number distribution
2 and the relative abundance of molecular families are significantly different. The chemical
3 composition of the samples is compared in terms of molecular family and carbon numbers as
4 shown in Figure 6. Determined compositions are presented in Table S1 and Table S3 with the
5 measurement uncertainty (Table S2 and Table S4) in the Supplementary Information.

6 **Figure 6.** Detailed chemical composition by molecular family and carbon number of N-PFO and
7 V-PFO. Molecular families identification and legends can be seen at the top right corner. Results
8 correspond to the average of three repeated injections, and error bars represent twice the standard
9 deviation.

10 Generally, PFO can be used for isolating basic aromatic chemicals as the carbon content (see
11 Table 2) and the concentration of PAHs (see Table 6) is similar to the one reported for
12 traditionally used coal tar⁵⁰. Extraction of diaromatics is particularly interesting as they are the
13 most abundant molecules in both samples, present in similar quantities, *i.e.* 28.6 wt.% for N-PFO
14 and 27.8 wt.% for V-PFO. The concentration of naphthalene, which is considered as a valuable
15 intermediate⁶⁰ in the chemical industry, is 12.5 wt.% in N-PFO, thus higher compared to the
16 concentration in coal tar. Additionally, PFO does not contain phenols and benzo[b]thiophene
17 which are usual contaminants after primary distillation of coal tar⁶⁰. Furthermore, production of
18 solvents, heat transfer oils, heat-resistant polyester fibers and pharmaceutical intermediates
19 requires C₁₁-C₁₃ diaromatics, which are present in considerable quantities in both N-PFO and V-
20 PFO (see Figure 6). However, due to the normal and wide distribution of molecules with side
21 chains in V-PFO, separation of pure chemicals is not obvious.

22 **Table 6.** Comparison of PAHs concentration in N-PFO and V-PFO.

1 N-PFO is richer in smaller molecules, such as naphthenoaromatics (18.6 wt.%) than V-PFO (9.7
2 wt.%). The measured amount of monoaromatics is similar, *i.e.* 16.4 wt.% and 16.9 wt.% for N-
3 PFO and V-PFO, respectively. Nonetheless, it should be noted that direct comparison of
4 aromatic compounds with low boiling point, *i.e.* molecules with carbon number from C₆ to C₉
5 should be done with care because of the partial evaporation of these molecules during the sample
6 preparation step (see section 2.4). V-PFO has a higher concentration of molecules belonging to
7 the heavier molecular families. The most noticeable differences arise from the amount of
8 triaromatics with a concentration of 14.8 wt.% and 5.6 wt.% for V-PFO and N-PFO,
9 respectively. Similarly, the concentration of naphthenotriaromatics and tetraaromatics in V-PFO,
10 4.4 wt.% and 4.2 wt.%, respectively, is higher compared to the concentrations in N-PFO, 1.5
11 wt.% and 1.5 wt.%, respectively.

12 Even though the carbon number distribution varies for the same molecular family for different
13 samples and for different molecular families within the same sample, some patterns can be
14 recognized. A normal distribution of molecules within each molecular family is clearly visible
15 for the V-PFO. The aliphatic side chains bonded to the aromatic core, *i.e.* di-, tri- and
16 tetraaromatics, and cores that are not completely aromatized, *i.e.* naphtheno-, naphthenodi- and
17 naphthenotriaromatics, are thus only mildly cracked. On the other hand, the purely aromatic
18 molecules, *e.g.* naphthalene for diaromatics, phenanthrene and anthracene for triaromatics, are
19 present in the highest concentration in N-PFO. Furthermore, the concentration of compounds
20 with a longer side chain gradually decreases within these two families. A similar trend is found
21 for tetraaromatics, however these compounds are tentatively identified due to the increased
22 number of isomers. These findings support the conclusion that both the nature of the feedstock

1 and the cracking temperature affect the ratio between aromatic and aliphatic carbon in the PFO
2 as concluded from ¹³C NMR results.

3 The high content of poly-aromatic molecules reduces the stability and furthermore increases the
4 viscosity making utilization of PFO as industrial fuel challenging. The drawbacks can be
5 overcome by thermal processing, *e.g.* visbreaking or coking, where PFO would be converted to
6 gas and lower viscosity liquid product. Production of gas would be favored during conversion of
7 V-PFO due to cracking of plentifully present aliphatic carbon bonded to aromatic and naphthenic
8 structures. On the other hand, the gas oil product would be favored during conversion of N-PFO
9 as a result of higher concentration of lower boiling point compounds, primarily
10 naphthenoaromatics. Poly-aromatic molecules would, however, lead to the formation of large
11 radicals that are coke formation precursors⁶¹, therefore coke formation would be substantial
12 making the process less attractive. Similar issues can be encountered during thermal catalytic
13 cracking due to extensive fouling on the metal catalyst^{7, 61}.

14 On the other hand, the abundance of poly-aromatics (see Table 6), *i.e.* PAHs makes blending of
15 PFO with other petroleum streams not straightforward. More specifically, PAHs are recognized
16 as air and food pollutants⁶², thus their maximal allowable concentration in petroleum products is
17 regulated⁶³. Thereby, the quality of the PFO should be increased through hydro-processing
18 before blending. Hydrotreating and hydrocracking processes would decrease the amount of poly-
19 aromatics and heavy naphthenoaromatic molecules, while increasing the content of
20 monoaromatics⁶⁴ and saturates in the product stream⁶⁵. The higher content of smaller molecules
21 in N-PFO, monoaromatics and naphthenoaromatics, would result in lower boiling point products,
22 however the treatment could be economically unjustifiable due to the low amount of PFO

1 produced during naphtha steam cracking. Nevertheless, the high V-PFO yields suggests
2 hydrotreating or hydrocracking as a possible processing steps for stream valorization.

3 These detailed compositional characterization results are the basis for assessing exploitation
4 possibilities and setting guidelines for process design. However, use of PFO as a feedstock for
5 the production of valuable chemicals or petroleum products primarily depends on economical
6 evaluation of conversion processes and regional market demands.

7 **4. CONCLUSIONS**

8 A variety of complementary analytical techniques have been used for improving the
9 understanding of the composition of the heaviest reaction products formed during steam cracking
10 of naphtha and VGO. Elemental compositions show relatively low molar H/C ratios, *i.e.* 0.95 for
11 N-PFO and 0.93 for V-PFO, which are lower than the ones typically reported for the asphaltene
12 fraction in Arabian crude oil. The high aromatic content of the produced fractions is confirmed
13 by NMR results, which shows the particularly large aromaticity of the PFO produced during
14 naphtha cracking. The lower dilution ratio and higher temperatures during naphtha compared to
15 VGO cracking promotes formation of heavier poly-aromatic cores and cracking of aliphatic
16 chains. The latter is indicated by the average aliphatic carbon chain length bonded to the
17 aromatic core. On the other hand, the increased presence of heavy aromatic cores is verified
18 through SARA fractionation that shows a larger concentration of n-hexane insolubles, *i.e.*
19 asphaltenes and coke, in N-PFO (19.5 wt.%) compared to V-PFO (10.3 wt.%). Due to the
20 significant concentration of n-hexane insolubles, so-called asphaltenes and coke, it is not
21 possible to completely characterize samples using GC × GC. The optimized GC × GC method
22 enables quantitative characterization of heavy poly-aromatic with boiling point up to 809 K.

1 Diaromatics are the most abundant molecular families in both PFO's with concentrations up to
2 29 wt.%. Also naphthenoaromatics are present in significant concentrations in N-PFO (19 wt.%),
3 while triaromatics are more characteristic for V-PFO (15 wt.%) because of the larger quantities
4 of these tricyclics in the original feed. These aromatic molecules together with asphaltenes
5 contribute to the fouling tendency of the PFO, thus hydro-conversion is required for further
6 valorization of PFO either as a feedstock or as a fuel.

7 ASSOCIATED CONTENT

8 Procedure for calculation of the mass fractions of the detected compounds by GC \times GC-
9 FID/TOF-MS is described in the Supplementary Information. Moreover, the composition of both
10 N-PFO and V-PFO expressed by molecular family and carbon number is reported in Table S1
11 and Table S3, respectively. Standard deviations of the GC \times GC-FID measurements are given in
12 Table S2 and Table S4. Finally, an interested reader can find a schematic description of the pilot
13 plant steam cracker in Figure S1 of Supplementary Information.

14 AUTHOR INFORMATION

15 **Corresponding Author**

16 *Kevin M. Van Geem

17 Laboratory for Chemical Technology (LCT), Ghent University

18 Technologiepark 918, B-9052, Ghent Belgium

19 Tel.:+3292645677

20 E-mail address: Kevin.VanGeem@Ugent.be

1 **Notes**

2 The authors declare no competing financial interest.

3 **Author Contributions**

4 The manuscript was written through contributions of all authors. All authors have given approval
5 to the final version of the manuscript.

6 **SAFETY**

7 Do not forget that working with poly-nuclear aromatic hydrocarbons, dichloromethane, carbon
8 disulfide, deuterated chloroform and n-hexane can be extremely hazardous, thus samples should
9 be prepared and kept in well-ventilated areas.

10 **ACKNOWLEDGMENTS**

11 This work was supported by the 'Long Term Structural Methusalem Funding by the Flemish
12 Government' and the European Union Horizon H2020 Programme (H2020-SPIRE-04-2016) under
13 grant agreement n°723706.

14

15 **ABBREVIATIONS**

16	PFO	Pyrolysis Fuel Oil
17	VGO	Vacuum Gas Oil
18	N – PFO	Naphtha Pyrolysis Fuel Oil
19	V – PFO	Vacuum Gas Oil Pyrolysis Fuel Oil
20	GC × GC	Comprehensive Two Dimensional Gas Chromatography
21	NMR	Nuclear Magnetic Resonance
22	FID	Flame Ionization Detector
23	TOF – MS	Time-of-Flight Mass Spectrometer

1	H/C	Molar Hydrogen-to-Carbon ratio
2	PAH	Poly-nuclear Aromatic Hydrocarbons
3	TLE	Transfer Line Heat Exchanger
4	CDCl ₃	Deuterated Chloroform
5	DCM	Dichloromethane
6	SARA	Saturates, Aromatics, Resins and Asphaltenes
7	DIP – MS	Direct Insertion Probe-Mass Spectrometry
8	FT – ICR – MS	Fourier Transform Ion Cyclotron Resonance Mass Spectrometry
9	HPLC	High-performance liquid chromatography
10	CHNS & O	Carbon, Hydrogen, Nitrogen, Sulfur, and Oxygen
11	PINA	Paraffins, Isoparaffins, Naphthenes, Aromatics
12	EA	Elemental Analyzer
13	MPLC	Mid-pressure Liquid Chromatography
14	FAA	Fraction of Aromatic carbons with Attachments
15	Cn'	Average aliphatic Carbon chain length

16

17 REFERENCES

- 18 1. Froment, G. F. Kinetics and reactor design in the thermal-cracking for olefins production. *Chem.*
19 *Eng. Sci.* **1992**, 47, (9-11), 2163-2177.
- 20 2. Lederer, J.; Ohanka, V.; Fulin, P.; Sebor, G.; Blazek, J. A study of industrial pyrolysis of the
21 high-boiling products from hydrocracking of petroleum vacuum distillate. *Fuel* **1994**, 73, (2), 295-
22 299.
- 23 3. Sebor, G.; Blazek, J.; Lederer, J.; Ricanek, M.; Novak, V. Pyrolysis of high-boiling petroleum
24 fractions. *Fuel* **1992**, 71, (11), 1231-1237.
- 25 4. Sebor, G.; Blazek, J.; Lederer, J.; Bajus, M. Pyrolysis of high-boiling product fractions from
26 petroleum vacuum distillate hydrocracking. *Fuel Process. Technol.* **1994**, 40, (1), 49-59.

- 1 5. Khani, M. R.; Guy, E. D.; Gharibi, M.; Shahabi, S. S.; Khosravi, A.; Norouzi, A. A.; Shokri, B.
2 The effects of microwave plasma torch on the cracking of Pyrolysis Fuel Oil feedstock. *Chem.*
3 *Eng. J.* **2014**, 237, 169-175.
- 4 6. Kim, H. G.; Park, M.; Kim, H.-Y.; Kwac, L. K.; Shin, H. K. Characterization of pitch prepared
5 from pyrolysis fuel oil via electron beam irradiation. *Radiat. Phys. Chem.* **2017**, 135, 127-132.
- 6 7. Upare, D. P.; Park, S.; Kim, M. S.; Kim, J.; Lee, D.; Lee, J.; Chang, H.; Choi, W.; Choi, S.;
7 Jeon, Y. P.; Park, Y. K.; Lee, C. W. Cobalt promoted Mo/beta zeolite for selective hydrocracking
8 of tetralin and pyrolysis fuel oil into monocyclic aromatic hydrocarbons. *J. Ind. Eng. Chem.* **2016**,
9 35, 99-107.
- 10 8. Mayani, V. J.; Mayani, S. V.; Lee, Y.; Park, S.-K. A non-chromatographic method for the
11 separation of highly pure naphthalene crystals from pyrolysis fuel oil. *Sep. Purif. Technol.* **2011**,
12 80, (1), 90-95.
- 13 9. Rammler, R. Pyrolysis-theory and industrial practice - Albright, L. F., Crynes, B. L., *Corcoran*
14 *W.H. Angewandte Chemie-International Edition in English* **1984**, 23, (9), 743-743.
- 15 10. Van Geem, K. M.; Reyniers, M. F.; Marin, G. B. Challenges of modeling steam cracking of
16 heavy feedstocks. *Oil & Gas Science and Technology-Revue D Ifp Energies Nouvelles* **2008**, 63,
17 (1), 79-94.
- 18 11. Kopinke, F. D.; Bach, G.; Zimmermann, G. New results about the mechanism of TLE fouling
19 in steam crackers. *J. Anal. Appl. Pyrolysis* **1993**, 27, (1), 45-55.
- 20 12. Wang, R. W.; Liu, G. J.; Zhang, J. M.; Chou, C. L.; Liu, J. J. Abundances of Polycyclic
21 Aromatic Hydrocarbons (PAHs) in 14 Chinese and American Coals and Their Relation to Coal
22 Rank and Weathering. *Energy & Fuels* **2010**, 24, 6061-6066.

- 1 13. Joshi, P. V.; Kumar, A.; Mizan, T. I.; Klein, M. T. Detailed Kinetic Models in the Context of
2 Reactor Analysis: Linking Mechanistic and Process Chemistry. *Energy & Fuels* **1999**, 13, (6),
3 1135-1144.
- 4 14. Ghosh, P.; Jaffe, S. B. Detailed composition-based model for predicting the cetane number of
5 diesel fuels. *Ind. Eng. Chem. Res.* **2006**, 45, (1), 346-351.
- 6 15. Flego, C.; Zannoni, C. Direct Insertion Probe-Mass Spectrometry (DIP-MS) Maps and
7 Multivariate Analysis in the Characterization of Crude Oils. *Energy & Fuels* **2013**, 27, (1), 46-55.
- 8 16. Flego, C.; Carati, C.; Del Gaudio, L.; Zannoni, C. Direct Mass Spectrometry of tar sands: A
9 new approach to bitumen identification. *Fuel* **2013**, 111, 357-366.
- 10 17. Flego, C.; Zannoni, C. Direct Insertion Probe-Mass Spectrometry: A Useful Tool for
11 Characterization of Asphaltenes. *Energy & Fuels* **2010**, 24, 6041-6053.
- 12 18. Schoenmakers, P. J.; Oomen, J.; Blomberg, J.; Genuit, W.; van Velzen, G. Comparison of
13 comprehensive two-dimensional gas chromatography and gas chromatography - mass
14 spectrometry for the characterization of complex hydrocarbon mixtures. *J. Chromatogr. A* **2000**,
15 892, (1-2), 29-46.
- 16 19. Zhao, Y.; Hong, B.; Fan, Y. Q.; Wen, M.; Han, X. Accurate analysis of polycyclic aromatic
17 hydrocarbons (PAHs) and alkylated PAHs homologs in crude oil for improving the gas
18 chromatography/mass spectrometry performance. *Ecotoxicol. Environ. Saf.* **2014**, 100, 242-250.
- 19 20. Cavagnino, D.; Magni, P.; Zilioli, G.; Trestianu, S. Comprehensive two-dimensional gas
20 chromatography using large sample volume injection for the determination of polynuclear
21 aromatic hydrocarbons in complex matrices. *J. Chromatogr. A* **2003**, 1019, (1-2), 211-220.

- 1 21. Phillips, J. B.; Beens, J. Comprehensive two-dimensional gas chromatography: a hyphenated
2 method with strong coupling between the two dimensions. *J. Chromatogr. A* **1999**, 856, (1-2), 331-
3 347.
- 4 22. Phillips, J. B.; Xu, J. Z. Comprehensive multidimensional gas-chromatography. *J.*
5 *Chromatogr. A* **1995**, 703, (1-2), 327-334.
- 6 23. Dalluge, J.; Beens, J.; Brinkman, U. A. T. Comprehensive two-dimensional gas
7 chromatography: a powerful and versatile analytical tool. *J. Chromatogr. A* **2003**, 1000, (1-2), 69-
8 108.
- 9 24. Dutriez, T.; Courtiade, M.; Thiebaut, D.; Dulot, H.; Bertoncini, F.; Vial, J.; Hennion, M. C.
10 High-temperature two-dimensional gas chromatography of hydrocarbons up to nC(60) for analysis
11 of vacuum gas oils. *J. Chromatogr. A* **2009**, 1216, (14), 2905-2912.
- 12 25. Dutriez, T.; Courtiade, M.; Thiebaut, D.; Dulot, H.; Hennion, M. C. Improved hydrocarbons
13 analysis of heavy petroleum fractions by high temperature comprehensive two-dimensional gas
14 chromatography. *Fuel* **2010**, 89, (9), 2338-2345.
- 15 26. Boursier, L.; Souchon, V.; Dartiguelongue, C.; Ponthus, J.; Courtiade, M.; Thiebaut, D.
16 Complete elution of vacuum gas oil resins by comprehensive high-temperature two-dimensional
17 gas chromatography. *J. Chromatogr. A* **2013**, 1280, 98-103.
- 18 27. Koolen, H. H. F.; Swarthout, R. F.; Nelson, R. K.; Chen, H.; Krajewski, L. C.; Aeppli, C.;
19 McKenna, A. M.; Rodgers, R. P.; Reddy, C. M. Unprecedented Insights into the Chemical
20 Complexity of Coal Tar from Comprehensive Two-Dimensional Gas Chromatography Mass
21 Spectrometry and Direct Infusion Fourier Transform Ion Cyclotron Resonance Mass
22 Spectrometry. *Energy & Fuels* **2015**, 29, (2), 641-648.

- 1 28. Stanford, L. A.; Kim, S.; Rodgers, R. P.; Marshall, A. G. Characterization of compositional
2 changes in vacuum gas oil distillation cuts by electrospray ionization Fourier transform-ion
3 cyclotron resonance (FT-ICR) mass spectrometry. *Energy & Fuels* **2006**, 20, (4), 1664-1673.
- 4 29. Sugumaran, V.; Biswas, H.; Yadav, A.; Christopher, J.; Kagdiyal, V.; Patel, M. B.; Basu, B.
5 Molecular-Level Characterization of Refinery Streams by High-Resolution Mass Spectrometry.
6 *Energy & Fuels* **2015**, 29, (5), 2940-2950.
- 7 30. Chacon-Patino, M. L.; Blanco-Tirado, C.; Orrego-Ruiz, J. A.; Gomez-Escudero, A.;
8 Combariza, M. Y. Tracing the Compositional Changes of Asphaltenes after Hydroconversion and
9 Thermal Cracking Processes by High-Resolution Mass Spectrometry. *Energy & Fuels* **2015**, 29,
10 (10), 6330-6341.
- 11 31. Xu, C.; Chen, H. M.; Sugiyama, Y.; Zhang, S. J.; Li, H. P.; Ho, Y. F.; Chuang, C. Y.; Schwehr,
12 K. A.; Kaplan, D. I.; Yeager, C.; Roberts, K. A.; Hatcher, P. G.; Santschi, P. H. Novel molecular-
13 level evidence of iodine binding to natural organic matter from Fourier transform ion cyclotron
14 resonance mass spectrometry. *Sci. Total Environ.* **2013**, 449, 244-252.
- 15 32. Muller, H.; Adam, F. M.; Panda, S. K.; Al-Jawad, H. H.; Al-Hajji, A. A. Evaluation of
16 Quantitative Sulfur Speciation in Gas Oils by Fourier Transform Ion Cyclotron Resonance Mass
17 Spectrometry: Validation by Comprehensive Two-Dimensional Gas Chromatography. *J. Am. Soc.*
18 *Mass. Spectrom.* **2012**, 23, (5), 806-815.
- 19 33. Clough, A.; Sigle, J. L.; Jacobi, D.; Sheremata, J.; White, J. L. Characterization of Kerogen
20 and Source Rock Maturation Using Solid-State NMR Spectroscopy. *Energy & Fuels* **2015**, 29,
21 (10), 6370-6382.
- 22 34. Kelemen, S. R.; Afeworki, M.; Gorbaty, M. L.; Sansone, M.; Kwiatek, P. J.; Walters, C. C.;
23 Freund, H.; Siskin, M.; Bence, A. E.; Curry, D. J.; Solum, M.; Pugmire, R. J.; Vandenbroucke,

- 1 M.; Leblond, M.; Behar, F. Direct characterization of kerogen by x-ray and solid-state C-13
2 nuclear magnetic resonance methods. *Energy & Fuels* **2007**, 21, (3), 1548-1561.
- 3 35. Bagley, S. P.; Wornat, M. J. Identification of Five- to Seven-Ring Polycyclic Aromatic
4 Hydrocarbons from the Supercritical Pyrolysis of n-Decane. *Energy & Fuels* **2011**, 25, (10), 4517-
5 4527.
- 6 36. Bagley, S. P.; Wornat, M. J. Identification of Six- to Nine-Ring Polycyclic Aromatic
7 Hydrocarbons from the Supercritical Pyrolysis of n-Decane. *Energy & Fuels* **2013**, 27, (3), 1321-
8 1330.
- 9 37. Poddar, N. B.; Thomas, S.; Wornat, M. J. Polycyclic aromatic hydrocarbons from the co-
10 pyrolysis of 1,3-butadiene and propyne. *Proceedings of the Combustion Institute* **2013**, 34, 1775-
11 1783.
- 12 38. Thomas, S.; Wornat, M. J. Polycyclic aromatic hydrocarbons from the co-pyrolysis of catechol
13 and 1,3-butadiene. *Proceedings of the Combustion Institute* **2009**, 32, 615-622.
- 14 39. Dijkmans, T.; Djokic, M. R.; Van Geem, K. M.; Marin, G. B. Comprehensive compositional
15 analysis of sulfur and nitrogen containing compounds in shale oil using GC x GC -
16 FID/SCD/NCD/TOF-MS. *Fuel* **2015**, 140, 398-406.
- 17 40. Van Geem, K. M.; Pyl, S. P.; Reyniers, M. F.; Vercammen, J.; Beens, J.; Marin, G. B. On-line
18 analysis of complex hydrocarbon mixtures using comprehensive two-dimensional gas
19 chromatography. *J. Chromatogr. A* **2010**, 1217, (43), 6623-6633.
- 20 41. Dhuyvetter, I.; Reyniers, M. F.; Froment, G. F.; Marin, G. B.; Viennet, D. The influence of
21 dimethyl disulfide on naphtha steam cracking. *Ind. Eng. Chem. Res.* **2001**, 40, (20), 4353-4362.
- 22 42. Ristic, N. D.; Djokic, M. R.; Van Geem, K. M.; Marin, G. B. On-line Analysis of Nitrogen
23 Containing Compounds in Complex Hydrocarbon Matrixes. *J. Vis. Exp.* **2016**, (114).

- 1 43. Zhang, Y.; Reyniers, P. A.; Schietekat, C. M.; Van Geem, K. M.; Marin, G. B.; Du, W. L.;
2 Qian, F. Computational fluid dynamics-based steam cracking furnace optimization using feedstock
3 flow distribution. *AIChE J.* **2017**, 63, (7), 3199-3213.
- 4 44. Solum, M. S.; Pugmire, R. J.; Grant, D. M. C-13 solid-state NMR of Argonne Premium Coals.
5 *Energy & Fuels* **1989**, 3, (2), 187-193.
- 6 45. Toraman, H. E.; Dijkmans, T.; Djokic, M. R.; Van Geem, K. M.; Marin, G. B. Detailed
7 compositional characterization of plastic waste pyrolysis oil by comprehensive two-dimensional
8 gas-chromatography coupled to multiple detectors. *J. Chromatogr. A* **2014**, 1359, 237-246.
- 9 46. Beens, J.; Janssen, H.-G.; Adahchour, M.; Brinkman, U. A. T. Flow regime at ambient outlet
10 pressure and its influence in comprehensive two-dimensional gas chromatography. *J. Chromatogr.*
11 *A* **2005**, 1086, (1), 141-150.
- 12 47. NIST. Mass Spectral Library and Other Tools. <http://www.chemdata.nist.gov>
- 13 48. Dijkmans, T.; Van Geem, K. M.; Djokic, M. R.; Marin, G. B. Combined Comprehensive Two-
14 Dimensional Gas Chromatography Analysis of Polyaromatic Hydrocarbons/Polyaromatic Sulfur-
15 Containing Hydrocarbons (PAH/PASH) in Complex Matrices. *Ind. Eng. Chem. Res.* **2014**, 53,
16 (40), 15436-15446.
- 17 49. Shirokoff, J. W.; Siddiqui, M. N.; Ali, M. F. Characterization of the structure of Saudi crude
18 asphaltene by X-ray diffraction. *Energy & Fuels* **1997**, 11, (3), 561-565.
- 19 50. Blümer, G.-P.; Collin, G.; Höke, H. Tar and Pitch. In Ullmann's Encyclopedia of Industrial
20 Chemistry, *Wiley-VCH Verlag GmbH & Co. KGaA*: **2000**.
- 21 51. Jung, M.-J.; Jung, J.-Y.; Lee, D.; Lee, Y.-S. A new pitch reforming from pyrolysis fuel oil by
22 UV irradiation. *Ind. Eng. Chem. Res.* **2015**, 22, 70-74.

- 1 52. Omais, B.; Courtiade, M.; Charon, N.; Thiebaut, D.; Quignard, A. Characterization of
2 Oxygenated Species in Coal Liquefaction Products. An Overview. *Energy & Fuels* **2010**, *24*, 5807-
3 5816.
- 4 53. Rodgers, R. P.; McKenna, A. M., Petroleum Analysis. *Anal. Chem.* **2011**, *83*, (12), 4665-4687.
- 5 54. Schietekat, C. M.; van Goethem, M. W. M.; Van Geem, K. M.; Marin, G. B. Swirl flow tube
6 reactor technology: An experimental and computational fluid dynamics study. *Chem. Eng. J.* **2014**,
7 238, 56-65.
- 8 55. Schietekat, C. M.; Van Cauwenberge, D. J.; Van Geem, K. M.; Marin, G. B. Computational
9 Fluid Dynamics-Based Design of Finned Steam Cracking Reactors. *AIChE J.* **2014**, *60*, (2), 794-
10 808.
- 11 56. Wiehe, I. A.; Liang, K. S. Asphaltenes, resins, and other petroleum macromolecules. *Fluid*
12 *Phase Equilib.* **1996**, *117*, (1-2), 201-210.
- 13 57. Lestina, T. G.; Zettler, H. U. Crude Oil Fouling Research: HTRI's Perspective. *Heat Transfer*
14 *Eng.* **2014**, *35*, (3), 217-223.
- 15 58. Fan, Z. M.; Rahimi, P.; McGee, R.; Wen, Q.; Alem, T. Investigation of Fouling Mechanisms
16 of a Light Crude Oil Using an Alcor Hot Liquid Process Simulator. *Energy & Fuels* **2010**, *24*,
17 6110-6118.
- 18 59. Giddings, J. C. Concepts and comparisons in multidimensional separation. *HRC CC J.* **1987**,
19 10, (5), 319-323.
- 20 60. Collin, G.; Höke, H.; Greim, H. Naphthalene and Hydronaphthalenes. In Ullmann's
21 Encyclopedia of Industrial Chemistry, *Wiley-VCH Verlag GmbH & Co. KGaA*: **2000**.
- 22 61. Sawarkar, A. N.; Pandit, A. B.; Samant, S. D.; Joshi, J. B. Petroleum residue upgrading via
23 delayed coking: A review. *Can. J. Chem. Eng.* **2007**, *85*, (1), 1-24.

1 62. Ravindra, K.; Sokhi, R.; Van Grieken, R. Atmospheric polycyclic aromatic hydrocarbons:
2 Source attribution, emission factors and regulation. *Atmos. Environ.* **2008**, 42, (13), 2895-2921.

3 63. Parliament, T. E., Directive 2009/30/EC. In **2009**; Vol. 2009/30/EC.

4 64. Upare, D. P.; Park, S.; Kim, M. S.; Jeon, Y. P.; Kim, J.; Lee, D.; Lee, J.; Chang, H.; Choi, S.;
5 Choi, W.; Park, Y. K.; Lee, C. W. Selective hydrocracking of pyrolysis fuel oil into benzene,
6 toluene and xylene over CoMo/beta zeolite catalyst. *J. Ind. Eng. Chem.* **2017**, 46, 356-363.

7 65. Dutriez, T.; Courtiade, M.; Thiebaut, D.; Dulot, H.; Borrás, J.; Bertoincini, F.; Hennion, M. C.
8 Advances in Quantitative Analysis of Heavy Petroleum Fractions by Liquid Chromatography-
9 High-Temperature Comprehensive Two-Dimensional Gas Chromatography: Breakthrough for
10 Conversion Processes. *Energy & Fuels* **2010**, 24, 4430-4438.

11
12
13
14
15
16
17
18
19
20
21
22
23

1 **Table 1.** Elemental composition, molecular family mass percentage and boiling point curve of
 2 naphtha and VGO.

Elemental Analysis	naphtha	VGO	ASTM-D1160 (K)	naphtha	VGO
Carbon (wt.%)	82.8 ± 0.06	87.62 ± 0.06	0%	296	400
Hydrogen (wt.%)	17.2 ± 0.05	12.3 ± 0.07	5%	316	527
Nitrogen (wt.%)	<0.01 ^a	<0.01 ^a	10%	319	548
Sulfur (wt.%)	<0.01 ^a	0.08 ± 0.02	20%	322	575
Oxygen (wt.%)	<0.01 ^a	<0.01 ^a	30%	326	592
H/C (mol/mol.)	2.49 ± 0.01	1.68 ± 0.01	40%	330	609
GC × GC	naphtha	VGO	50%	334	622
paraffins (wt.%)	36.40 ± 0.16	23.92 ± 0.31	60%	339	634
isoparaffins (wt.%)	38.85 ± 0.07	24.25 ± 0.61	70%	345	646
cycloalkanes (wt.%)	20.71 ± 0.04	17.60 ± 0.17	80%	352	661
aromatics (wt.%)	4.04 ± 0.02	33.33 ± 0.31	90%	360	675
bio-markers (wt.%)	<0.01 ^a	0.91 ± 0.02	95%	367	688
Carbon number	4 - 9	8-35	100%	371	740

3 a) below the detection limit of the method

4

5

1

Table 2. Comparison of the elemental composition of N-PFO and V-PFO.

	N-PFO	V-PFO	Coal tar ⁵⁰	Saudi Arabian asphaltenes ⁴⁹
Carbon (wt.%)	90.9 ± 0.4	91.8 ± 0.4	90 – 93	83.2 - 85
Hydrogen (wt.%)	7.2 ± 0.1	7.1 ± 0.1	5 – 6	7.2 – 8.28
Nitrogen (wt.%)	0.1 ± 0.03	0.1 ± 0.01	0.6 – 1.2	0.3 – 0.8
Sulfur (wt.%)	< 0.01 ^a	< 0.01 ^a	0.6 – 1.0	6.3 – 7.2
Oxygen (wt.%)	1.8 ± 0.1	1.0 ± 0.1	1.5 – 2.0	0.5 - 1.1
H/C (mol/mol)	0.95 ± 0.02	0.93 ± 0.02	0.69	1.02 – 1.19

2

a) below the detection limit of the method

3

Table 3. SARA fractionation results for N-PFO and V-PFO.

4

	N-PFO	V-PFO
Topping loss, wt.%	53.9 ± 0.5	28.7 ± 0.1
Saturates, wt.%	0.9 ± 0.1	0.5 ± 0.1
Aromatics, wt.%	16.5 ± 1.4	43.3 ± 0.2
Resins, wt.%	8.7 ± 0.5	14.1 ± 0.2
Asphaltenes & coke, wt.%	19.5 ± 0.5	10.3 ± 0.2

5

6

7

8

9

Reported values correspond to the average of two measurement, the associated uncertainty

10

indicates the difference with respect to the average.

11

1

Table 4. ^{13}C NMR determined structural and lattice parameters of N-PFO and V-PFO.

Structural parameter	chemical shift range (ppm)	N-PFO (wt.%)	V-PFO (wt.%)
aromatic (fa')	90-165	92.07 ± 0.07	89.01 ± 0.28
carboxyl/carbonyl/amide (fa^{C})	165-240	<0.3 ^a	<0.3 ^a
phenoxy/phenolic (fa^{P})	150-165	<0.3 ^a	<0.3 ^a
alkyl-substituted aromatic, biaryl (fa^{S})	135-150	7.14 ± 0.40	6.07 ± 0.27
aliphatic (fal)	0-90	7.93 ± 0.07	10.99 ± 0.29
methylene/methine (fal^{H})	22-90 – (50-60)	5.84 ± 0.30	6.05 ± 0.25
methyl (fal^*)	0-22	2.10 ± 0.37	4.94 ± 0.03
methoxy (fal^{mo})	50-60	<0.3 ^a	<0.3 ^a
alcohol/ether (fal^{O})	50-90	<0.3 ^a	<0.3 ^a
lattice parameter	definition	N-PFO	V-PFO
fraction of aromatic carbons with attachments (FAA)	$(\text{fa}^{\text{P}} + \text{fa}^{\text{S}}) / \text{fa}'$	0.08	0.07
average aliphatic carbon chain length (Cn')	$\text{fal} / \text{fa}^{\text{S}}$	1.11	1.81

2

Reported values correspond to the average of two measurements, the associated uncertainty

3

indicates the difference with respect to the average.

4

a) below the detection limit of the method

5

Table 5. Composition of the standard test mixture.

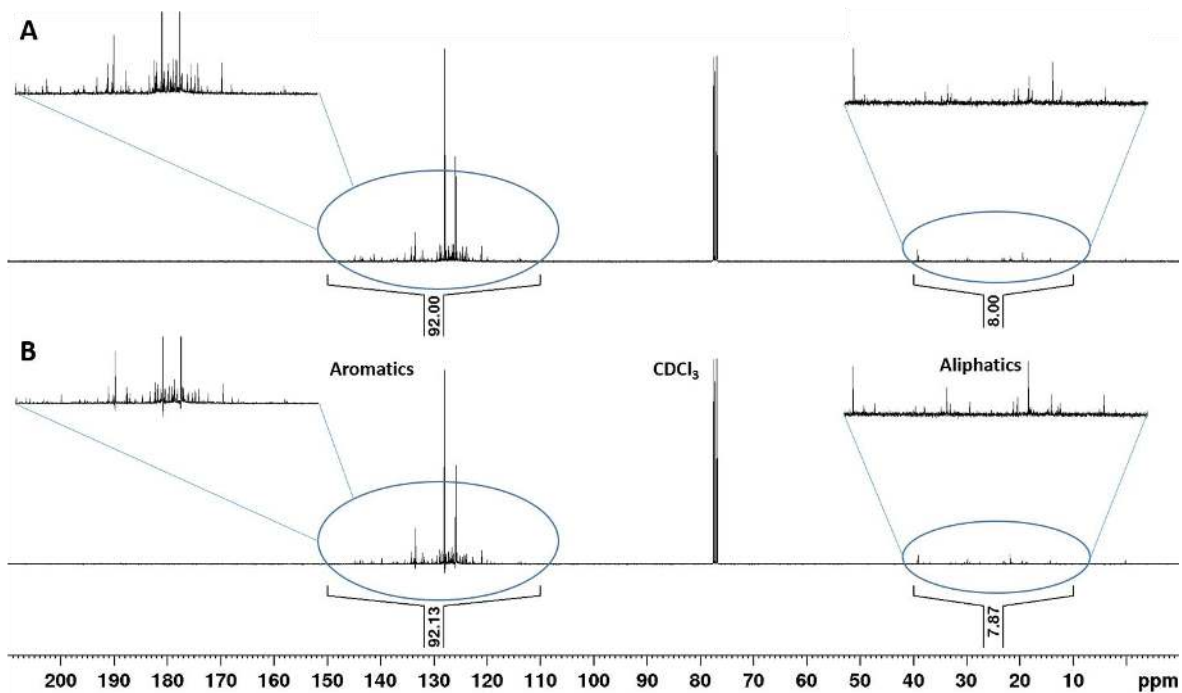
Assigned number in the chromatogram	Compound name
1	Naphthalene
2	1-Methylnaphthalene
3	2-Methylnaphthalene
4	Acenaphthene
5	Acenaphthylene
6	Fluorene
7	Phenanthrene
8	Anthracene
9	Fluoranthene
10	Pyrene
11	Benzo[a]anthracene
12	Chrysene
13	Benzo[k]fluoranthene
14	Benzo[b]fluoranthene

1	15	Benzo[a]pyrene
2	16	Benzo[ghi]perylene
3	17	Dibenz[a,h]anthracene
4		
5	18	Indeno[1,2,3-cd]pyrene

Table 6. Comparison of PAHs concentration in N-PFO and V-PFO.

Compound name	N-PFO	V-PFO	Coal Tar ⁵⁰
Naphthalene	12.5	3.8	10.0
1-Methylnaphthalene	2.1	2.2	0.7
2-Methylnaphthalene	3.7	3.3	1.5
Acenaphthene	0.4	0.2	0.2
Acenaphthylene	1.7	1.0	2.5
Fluorene	1.1	1.0	1.8
Phenanthrene	1.6	1.4	4.5
Anthracene	0.3	0.4	1.3
Fluoranthene	0.1	0.2	3.0
Pyrene	0.4	0.3	2.0
Chrysene	0.1	0.1	1.0

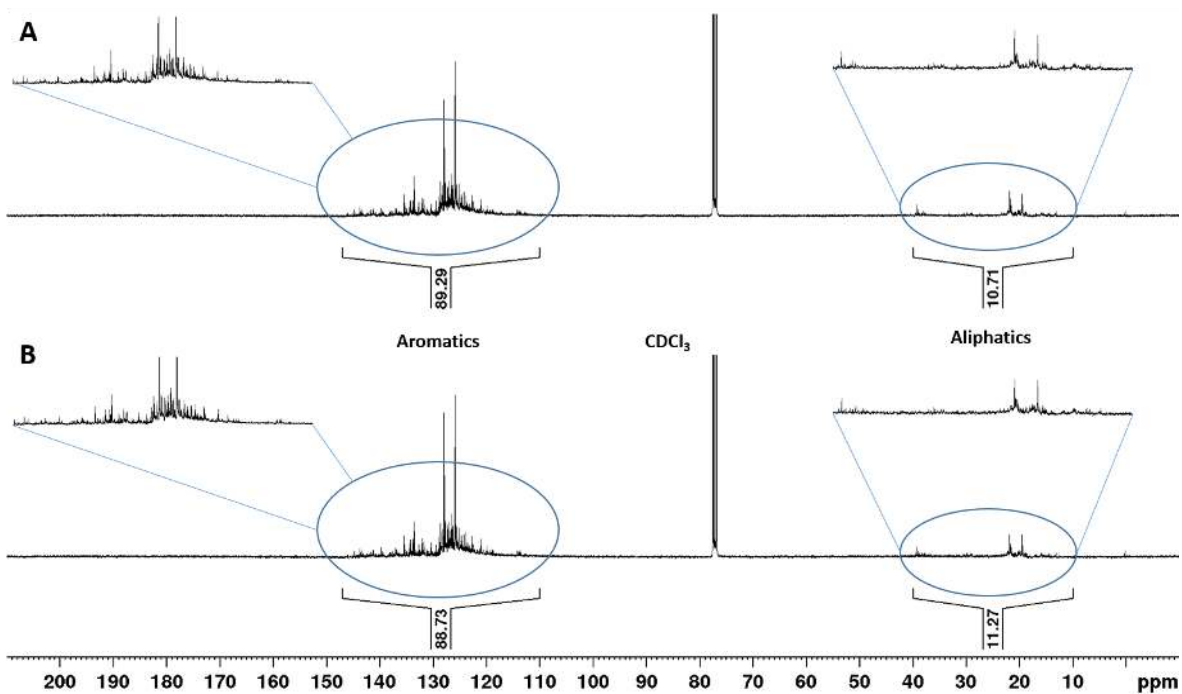
Results correspond to the average of three repeated injections.



1

2

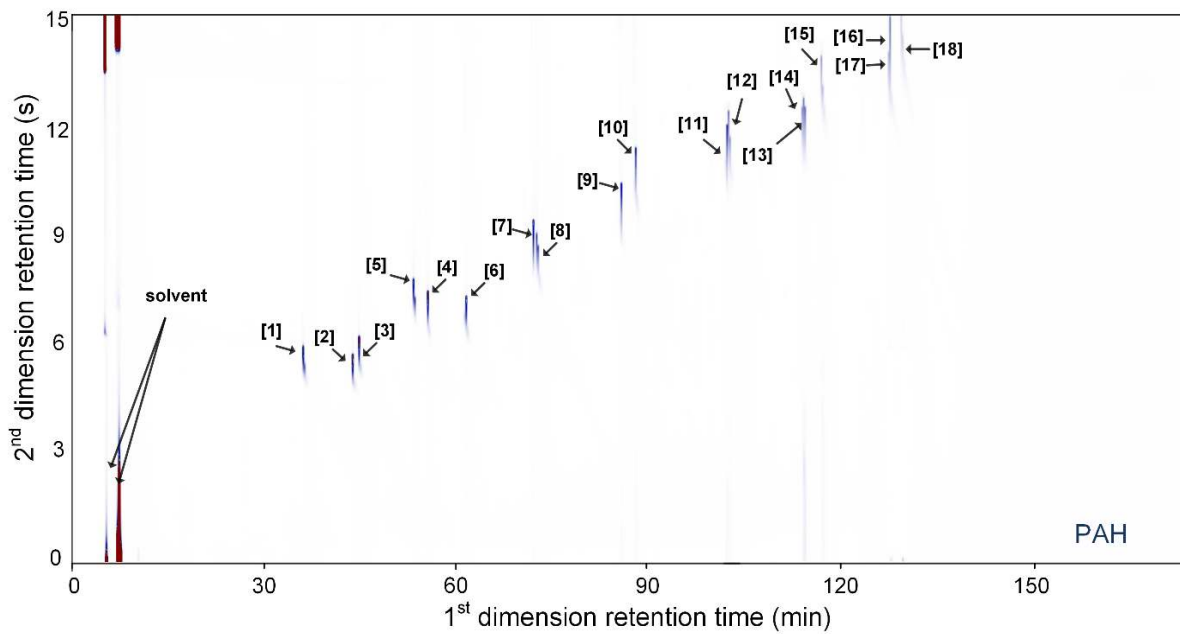
Figure 1. ^{13}C NMR spectrum of N-PFO.



3

4

Figure 2. ^{13}C NMR spectrum of V-PFO.

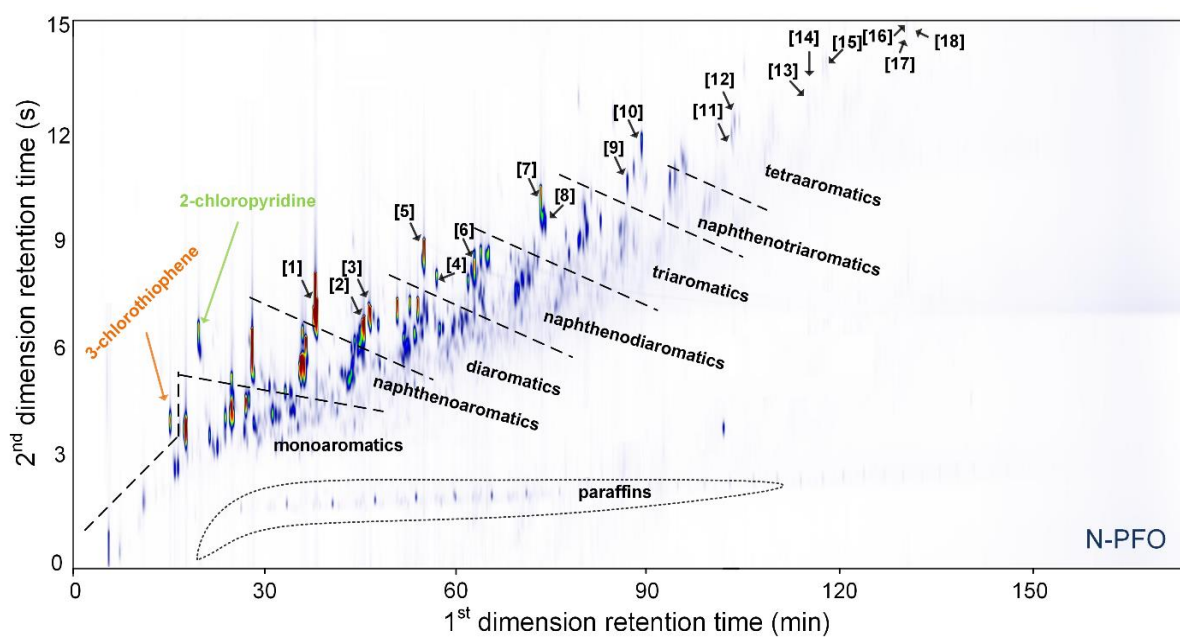


1

2

Figure 3. GC × GC-FID chromatogram of the PAH standard. Numbers correspond to the compounds list in Table 5.

3



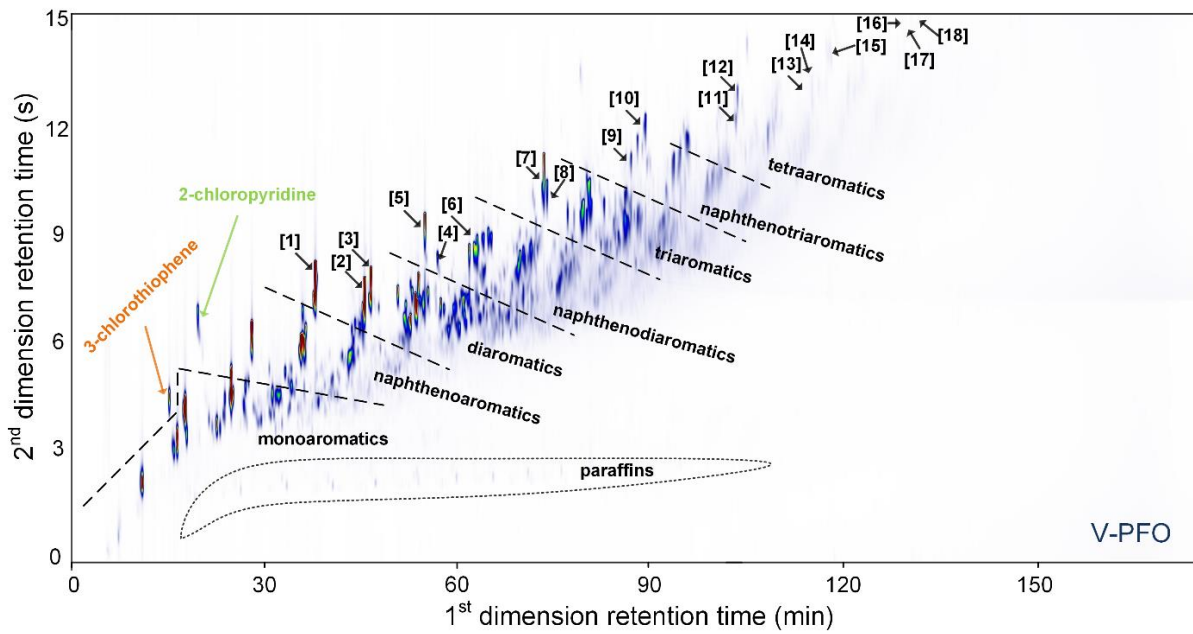
4

5

Figure 4. GC × GC-FID chromatogram of the N-PFO with separation of molecular families.

6

Numbers correspond to the compounds list in Table 5.

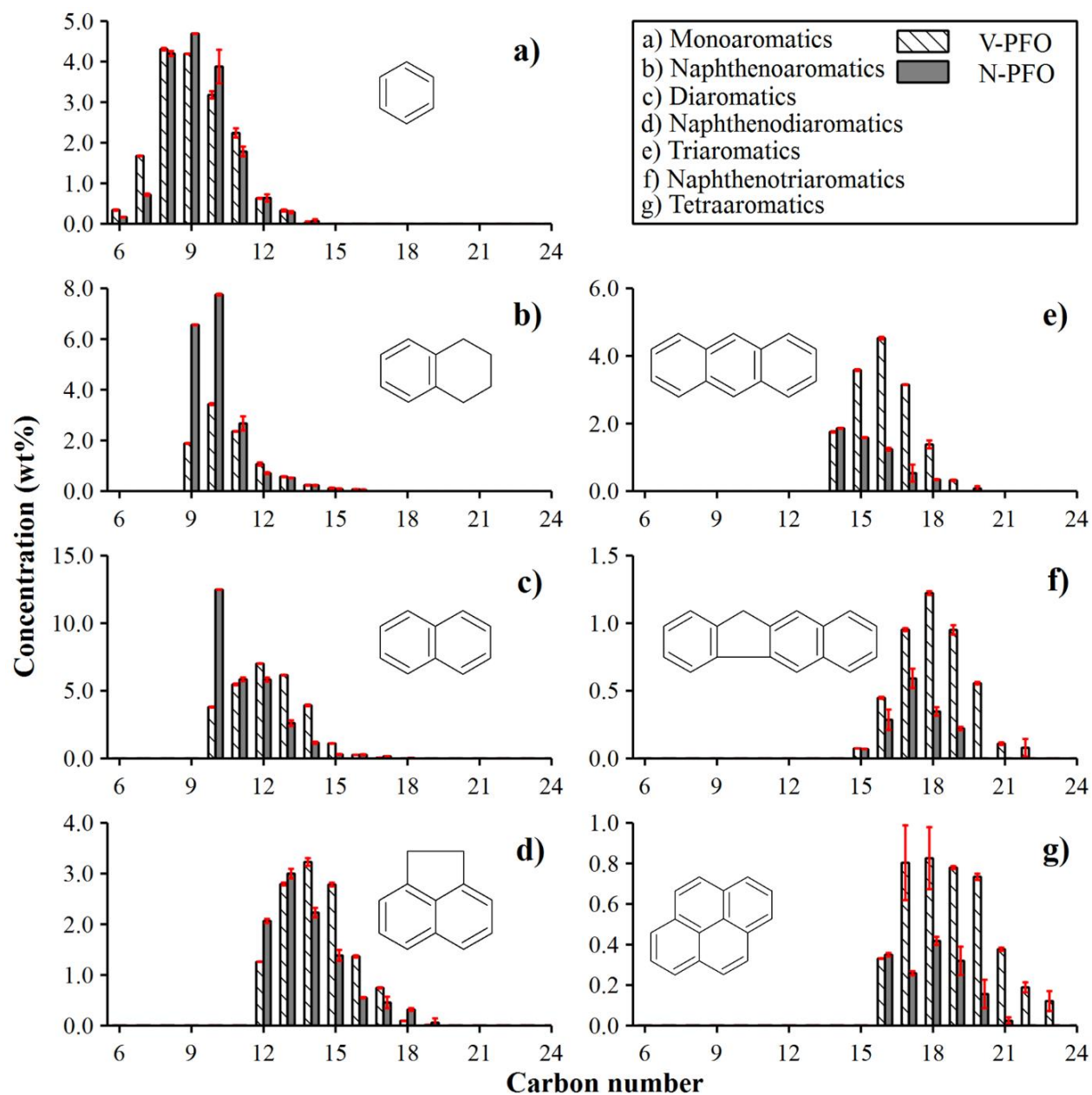


1

2 **Figure 5.** GC × GC-FID chromatogram of the V-PFO with separation of molecular families.

3

Numbers correspond to the compounds list in Table 5.



1
 2 **Figure 6.** Detailed chemical composition by molecular family and carbon number of N-PFO and
 3 V-PFO. Molecular families identification and legends can be seen at the top right corner. Results
 4 correspond to the average of three repeated injections, and error bars represent twice the standard
 5 deviation.
 6